



PDZRN4-mediated colon cancer cell proliferation and dissemination is regulated by miR-221-3p

Xiaojian Liu, Chungeng Xing

Department of General Surgery, The Second Affiliated Hospital of Soochow University, Suzhou 215004, China

Contributions: (I) Conception and design: C Xing; (II) Administrative support: None; (III) Provision of study materials or patients: None; (IV) Collection and assembly of data: X Liu; (V) Data analysis and interpretation: All authors; (VI) Manuscript writing: All authors; (VII) Final approval of manuscript: All authors.

Correspondence to: Chungeng Xing, Department of General Surgery, The Second Affiliated Hospital of Soochow University, Suzhou 215004, China. Email: xingcg@suda.edu.cn.

Background: Suppression of *PDZRN4* expression in colon cancer tissues may be associated with elevated levels of the microRNA 221 (miR-211). To uncover potential targets for treatment, the present study investigated *PDZRN4* in colon cancer development, and explored the role of miR-221-3p in the regulation of *PDZRN4*.

Methods: RNA expression arrays were searched in the NCBI database, and *PDZRN4* (PDZ domain containing ring finger 4) was selected as a potential downregulated gene in colon cancer. *PDZRN4* mRNA and protein in colon cancer and matched normal tissues were analyzed. The proliferation and dissemination of HCT116 cells overexpressing *PDZRN4* was assessed via functional assays. Bioinformatics analysis and luciferase reporter assay were applied to determine the regulatory link between miR-221-3p and *PDZRN4* mRNA.

Results: There was significantly less *PDZRN4* mRNA and *PDZRN4* protein in colon cancer tissue compared with normal tissues. HCT116 cells overexpressing *PDZRN4* were less able to disseminate relative to the control. Expression of *PDZRN4* was directly inhibited by miR-221-3p. Knockout of miR-211-3p was associated with attenuated proliferation and dissemination of HCT116 cells.

Conclusions: *PDZRN4* may function as a tumor suppressor and is downregulated in colon cancer tissues, possibly due to dysregulation via miR-221-3p. This study provides new insight into colon cancer development.

Keywords: PDZ domain containing ring finger 4 (*PDZRN4*); colon cancer; microRNA; 3'-untranslated region (3'-UTR); mRNA; proliferation

Submitted Feb 17, 2019. Accepted for publication Jun 24, 2019.

doi: 10.21037/tcr.2019.07.12

View this article at: <http://dx.doi.org/10.21037/tcr.2019.07.12>

Introduction

Despite rapid advances in diagnostic and treatment strategies, colon cancer still ranks high among commonly diagnosed cancers, and its incidence is rising (1). In China, the incidence in men and women is 16.9 and 11.6 per 100,000, respectively (2). Colon cancer is closely associated with other diseases such as diabetes and obesity, making it a major public health risk (3,4). Despite the rapid increase in newly diagnosed patients, the etiology and mechanism of

colon cancer development remains unclear.

The gene *PDZRN4* (PDZ domain containing ring finger 4) belongs to the ligand of numb protein-X (LNX) family and is dysregulated in multiple diseases, including radiation-induced papillary thyroid carcinoma, rectal adenocarcinoma, and hepatocellular carcinoma (5,6). In human liver cancer cell lines, the ectopic expression of *PDZRN4* inhibited cancer cell proliferation, as well as plate colony formation and anchorage-independent colony

formation (7). Analysis of gene expression data indicates that the gene *PDZRN4* is downregulated in colon cancer. In the present study, we investigated the role of *PDZRN4* in colon cancer development.

MicroRNAs (miRNAs) are a small noncoding RNA that, by binding to a coding sequence or 3'-untranslated region (UTR), can interfere with mRNA translation or stability, changing expression of the gene. Depending on its downstream gene, miRNAs can function as either tumor suppressors or oncogenes. Because miRNAs have such roles in the development of cancers (8-10), we wondered whether miRNAs may be implicated in the differential expression of *PDZRN4* in colon cancer.

Specifically, miR-221 is a putative regulator in tumor development (11-13), and according to open access data in the National Center for Biotechnology Information (NCBI) database its levels are usually elevated in colon cancer (GSE101502). In addition, higher level of miR-221 in colon cancer tissues is associated with poor prognosis (14,15). The expression of miR-221 is regulated by multiple regulators, including KRAS, NF- κ B (nuclear factor kappa-light-chain-enhancer of activated B cells), STAT3 (signal transducer and activator of transcription 3), and KRAP (Ki-ras-induced actin-interacting protein), while KRAP-regulated miR-221 expression could only be seen in a 3D culture, and NF- κ B and STAT3 activation is, in turn, manipulated by miR-221 expression (16,17).

It is possible that miRNAs can have multiple targets, and the link between miR-221 and *PDZRN4* remains unclear. To contribute information toward the diagnosis and treatment of colon cancer, the present study explored the potential regulation of *PDZRN4* by miR-221-3p.

Methods

Ethics statement

The Institutional Ethics Committee of Second Affiliated Hospital of Soochow University (Suzhou, 215004, Jiangsu Province, China) reviewed and authorized the clinical section of this research.

Colon cancer tissue samples

Twenty pairs of colon cancer tissues and adjacent normal tissues were collected from patients who received treatment in our hospital. None of the patients received radiotherapy or chemotherapy before surgery (Table S1).

All diagnoses were obtained via pathological examination. All examinations and evaluations of clinical samples were conducted using paired normal tissue as a control.

Cell line

Cells of the human colon cancer cell line, HCT116 were purchased from the American Type Culture Collection and cultured in RPMI-1640 medium (Gibco, Grand Island, NY, USA) containing 10% fetal bovine serum (FBS) (Gibco, Grand Island, NY, USA) at 37 °C, 5% CO₂.

293T cells were previously preserved in our lab and cultured in Dulbecco's modified Eagle's medium (Gibco, Grand Island, NY, USA) containing 10% FBS and 2 mM L-glutamine at 37 °C, 5% CO₂.

Cells were observed with a microscope (Olympus, Tokyo, Japan) and green fluorescent protein (GFP) was observed with a fluorescence microscope.

Plasmids

The pLVX-*PDZRN4* plasmid was constructed by inserting the *PDZRN4* coding sequence into the lentiviral expression vector, pLVX-IRES-ZsGreen1. The pLVX-miR-221-3p sponge was constructed by referring to a published article (18).

Immunohistochemistry (IHC)

The cancer tissues and paired adjacent normal tissues obtained from patients during surgery were processed for staining with hematoxylin and eosin and IHC. All the samples were formalin-fixed, paraffin-embedded, and immunostained with PDZRN4 antibody (ThermoFisher Scientific, Waltham, MA, USA). Quantification was conducted by counting the positive cells per field. Data is shown as mean \pm standard deviation (SD).

Western blot

Cells were lysed with sodium dodecyl sulfate (SDS) lysis buffer (Beyotime, China) and denaturalized in a water bath at 100 °C. The prepared protein was resolved via SDS-PAGE, transferred to a polyvinylidene difluoride membrane from Millipore, and incubated with PDZRN4 primary antibody and HRP-Goat Anti-Rabbit IgG (H + L) (MultiSciences, Hangzhou, China). Protein levels were detected with a peroxide LumiGLO reagent (Cell Signaling

Table 1 Primers used for RT-qPCR

Primers	Sequences
PDZRN4-forward	TTTGCCCTGGAGCGCTTCGCAGA
PDZRN4-reverse	CGCCTCCAGCTCGTGCAGCCTGA
miR-221-3p-forward	CAAGGAATCATGTATGCTGTAG
miR-221-3p-reverse	AGGATGACATTACACCTTATCTC
U6-forward	GCTTCGGCAGCACATATACTAAAAT
U6-reverse	CGCTTCACGAATTTGCGTGCAT

Technology, 7003). Quantification of the relative protein levels was conducted according to the ratio of gray-value to the corresponding internal references. A representative graph was constructed and protein was quantified based on five pairs of clinical samples or three independent experiments and shown as mean \pm SD.

Reverse transcription followed by real-time quantitative PCR (RT-qPCR)

RNA was extracted in accordance with the instructions for TRIzol reagent use (GENEray, Shanghai, China). The total RNA was subjected to reverse transcription using a kit from GENEray, Shanghai, China. Finally, cDNA was used for qPCR analysis. The RNA levels were normalized to internal references, and shown as mean \pm SD (for primers, *Table 1*).

Fluorescence-activated cell sorting (FACS, flow cytometry)

The rate of GFP-positive cells was determined using Accuri C6 (BD, San Jose, CA, USA). Cells were digested into single cells and determined by the GFP channel of Accuri C6. GFP-positive cells and the total cell number were counted automatically. The percentage of positive cells was calculated as positive cells number/total cell number \times 100%.

Cell proliferation assay using cell-counting kit 8 (CCK8)

Two thousand cells were suspended in 100- μ L culture medium and seeded per well in a 96-well plate; 8 plates were seeded. Each plate was collected daily after seeding, 10 μ L CCK8 solution (MultiSciences, Hangzhou, China) was added, and measurements were performed using a microplate reader at 450 nm; the first measurement was done a few hours after seeding. The relative proliferation rate is shown as mean \pm SD of reads at 450 nm.

Plate clone formation assay

One hundred cells were suspended in 2 mL culture medium in a 6-well plate. The medium was replenished every 2 days. The cell culture was observed daily until visible clones had formed. The culture medium was carefully removed and clones were stained with crystal violet solution. Data is shown as mean \pm SD of numbers of clones per field.

Migration and invasion assay

Cells were seeded to the upper chamber of Millicell hanging cell culture inserts (Merck Millipore, Darmstadt, Germany). Culture medium without FBS and complete culture medium, were added, respectively, to the upper and lower chambers of the culture wells. Cells that had migrated to the lower surface of the filter were fixed with 70% methanol and then stained with 0.5% crystal violet solution.

For the invasion assay, hanging cell culture inserts were pre-coated with diluted Matrigel an hour before cell seeding. The cells that migrated or invaded the lower surface of the wells were counted. Data are shown as mean \pm SD. Student's *t*-test was performed when comparing data between groups.

Wound-healing assay

Cells were seeded to six-well culture plates and cultured overnight. By the second day, the culture medium was carefully removed and medium pipette tips were used to scratch the monolayer cell culture. Floating cells were carefully removed and fresh medium was added to the cell culture.

Graphs were constructed at the time of the scratch (0 hour) and 12 hours after treatment.

The percentage of scratch remaining after wounding was calculated as: (measurement at 12 hours/measurement at 0 hour) \times 100%. The percentage of wound closure was calculated as: 100% – percentage of wound remaining. The percentage of wound closure is shown as mean \pm SD.

Statistical analysis

The data in this study are shown as mean \pm SD. The comparison of means between two groups was conducted using Student's *t*-test. $P < 0.05$ was considered significant; * $P < 0.05$, ** $P < 0.01$ and *** $P < 0.001$.

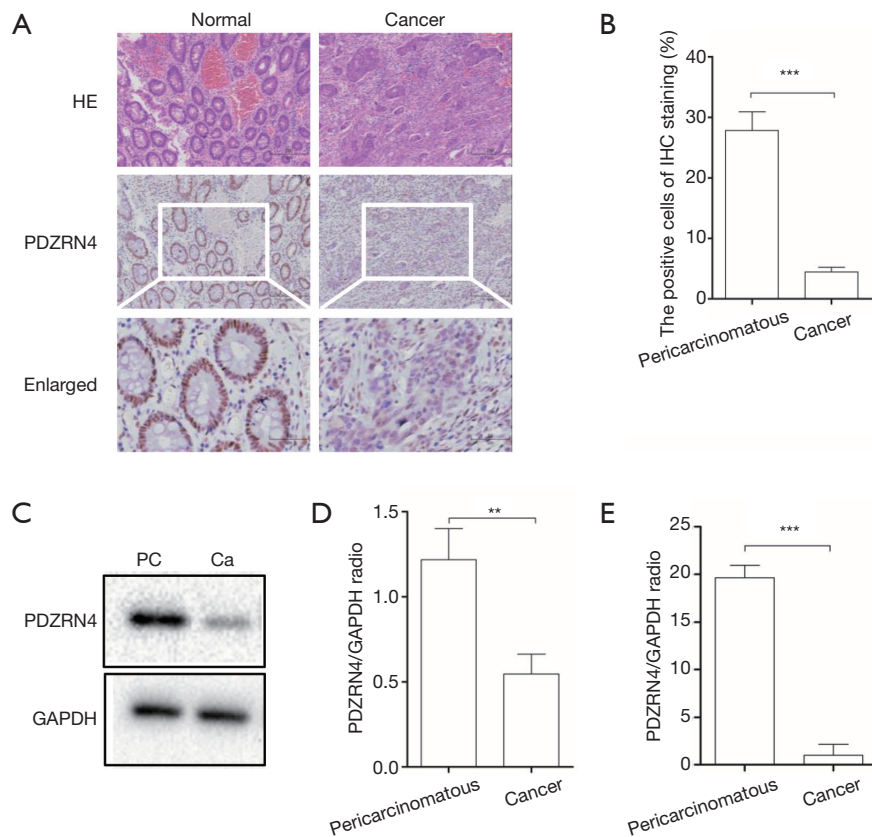


Figure 1 PDZRN4 expression is inhibited in colon cancer tissues. (A) PDZRN4 protein in normal colon tissue (left) and colon cancer tissue (right) revealed by IHC ($\times 100$ and $\times 400$ for enlarged). (B) Quantification of cells (as in *Figure 1A*) stained positive for PDZRN4 using normal tissue as the control. *** $P < 0.001$ for Student's *t*-test. (C) Western blot of PDZRN4 protein in five pairs of normal and cancer colon tissues. Ca, five colon cancer tissues; PC, matched normal tissues. (D) Quantification of PDZRN4 protein (see *Figure 1C*) using normal tissue as the control. ** $P < 0.01$ for Student's *t*-test. (E) mRNA levels of PDZRN4 in the same five pairs of normal and cancer colon tissues by RT-qPCR (see *Figure 1C*). *** $P < 0.001$ for Student's *t*-test.

Results

PDZRN4 is downregulated in colon cancer at both the mRNA and protein level

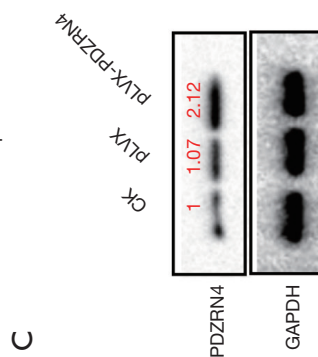
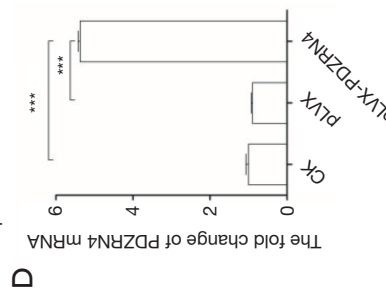
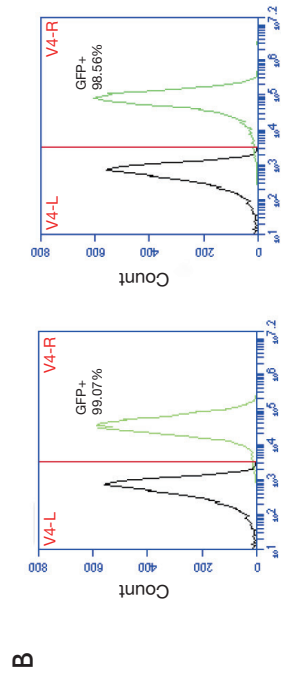
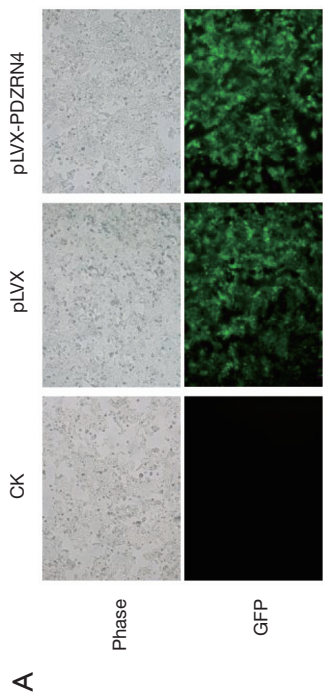
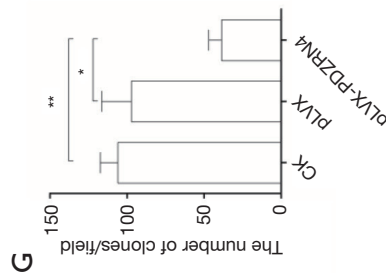
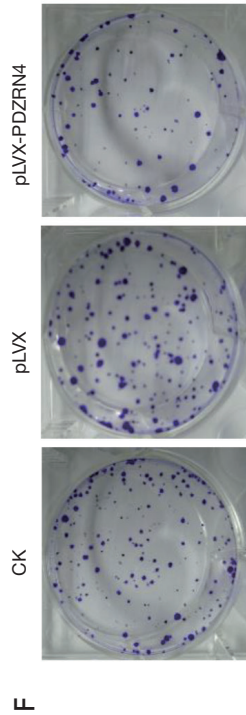
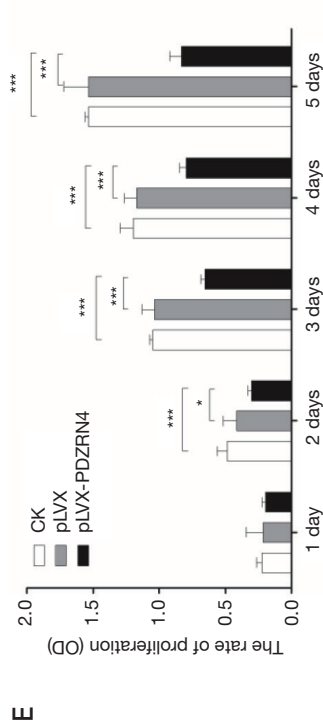
In the initial phase of this investigation, mRNA array data obtained from NCBI was analyzed (GEO accession: GSE75970 and GSE74604). We compared gene expression levels in both the array and screened differentially expressed gene, genes having a 2-fold difference in quantity between colon cancer tissues and normal tissues (*Figures S1, S2*). After searching studies and reports concerning differentially expressed genes, we found PDZRN4, downregulated in both arrays, had never been studied in colon cancer, and was not well illustrated in almost any disease.

The levels of PDZRN4 protein in 5 pairs of colon cancer tissues and matched normal tissues were compared using

IHC and western blot (*Figure 1A, B, C, D*). Both analyses showed lower amounts of PDZRN4 protein in the colon cancer tissues than in the normal tissues. In addition, RT-qPCR of 20 pairs of samples showed less *PDZRN4* mRNA in the cancer samples (*Figure 1E*). These results suggest that *PDZRN4* is suppressed at both the mRNA and translated levels in colon cancer.

Ectopic expression of PDZRN4 attenuated HCT116 cell's tumorigenesis

To determine if *PDZRN4* may be a regulator in colon cancer development, the gene was overexpressed in HCT116 cells (*Figure 2A*). The FACS, western blot, and RT-qPCR results confirmed the successful overexpression of *PDZRN4* (*Figure 2B, C, D*, respectively).



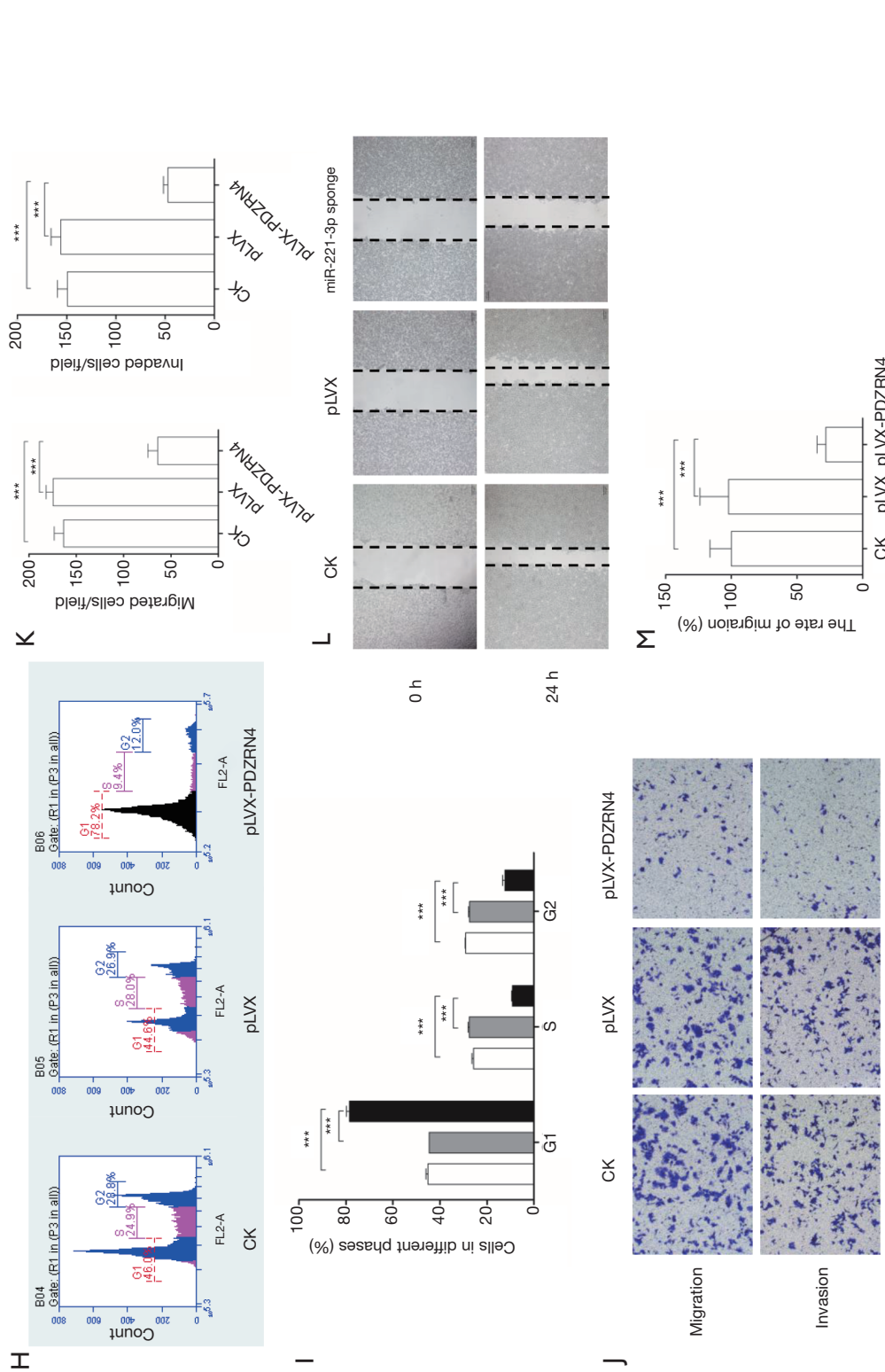


Figure 2 Overexpression of PDZRN4 inhibited the proliferation, migration, and invasion of HCT116 cells. (A) HCT116 cells were transfected with lentiviruses (middle) pLVX empty vector and (right) pLVX-PDZRN4. Representative images of (left) untreated cells, pLVX empty vector, or pLVX-PDZRN4 transfected cells were taken under (Phase, top) light microscope and (GFP, bottom) fluorescent microscope (100x). (B) Percentages of cells treated as in Figure 2A tested positive for GFP using FACS. (C) Western blot of PDZRN4 proteins in cells treated as in Figure 2A. (D) mRNA levels of PDZRN4 in cells treated as in Figure 2A. ***P<0.001 for Student's *t*-test. (E) Proliferation rates of cells treated as in Figure 2A by cell proliferation assay. *P<0.05, ***P<0.001 for Student's *t*-test. (F) Representative images for the clone formation assay of cells treated as in Figure 2A. (G) Numbers of clones formed (Figure 2F). *P<0.05, **P<0.01 for Student's *t*-test. (H) Percentage of cells treated as in Figure 2A in different cell cycle phases. (I) Percentages of cells in different cell phases. ***P<0.001 for Student's *t*-test. (J) Representative images for transwell migration and invasion of cells treated as in Figure 2A (100x). (K) Number of migrated and invaded cells per field. ***P<0.001 for Student's *t*-test. (L) Representative images of wound healing assay for cells treated as in Figure 2A (x100) ***P<0.001 for Student's *t*-test.

To investigate how *PDZRN4* regulates cancer cell activities, the cells overexpressing *PDZRN4* were then applied for functional assays. The cells overexpressing *PDZRN4* proliferated less compared with the control cells, as measured by the cell proliferation (*Figure 2E*) and plate clone formation (*Figure 2F,G*) assays. A study of the cell cycle of the transformed cells showed that fewer of those overexpressing *PDZRN4* reached S phase, compared with the control. This suggests that there was less DNA replication in the overexpressing cells (*Figure 2H,I*).

Tumor cells often have an enhanced ability to disseminate. In the present study, cells with overexpressed *PDZRN4* were much less able to disseminate via migration and invasion (*Figure 2J,K*), as also indicated by the wound healing assay (*Figure 2L,M*). Altogether, these data suggest that *PDZRN4* is suppressed in colon cancer, and this suppression promotes cancer cell proliferation and dissemination. Thus, *PDZRN4* may function as a tumor suppressor.

With this supposition, the regulation of *PDZRN4* expression in colon cancer was investigated.

PDZRN4 mRNA is a direct target of miR-221-3p

Since *PDZRN4* expression was dysregulated at both the mRNA and protein levels, we investigated whether it may be regulated by miRNAs. Thus, data from the noncoding RNA expression profile (GEO accession: GSE101501) was explored for implications in colon cancer. Using the databases RNAhybrid, TargetScanHuman, miRWalk, and miR, the following miRNAs listed as upregulated in colon cancer tissues in the databases were selected and investigated for binding potential with the *PDZRN4* 3'-UTR: miR-153-3p, miR-5195-3p, miR-371a-3p, miR-133a-5p, miR-221-3p, miR-31-5p, miR-373-3p, miR-615-5p, miR-582-3p, and miR-301b-3p. To determine the association of these miRNAs with *PDZRN4*, *PDZRN4* was measured after knocking out each miRNA respectively. It was found that, among these miRNAs, transfection with the miR-221-3p inhibitor was associated with dramatically higher levels of both protein *PDZRN4* and mRNA *PDZRN4* (*Figure 3A,B*).

To verify binding further, luciferase report assays were conducted. The results showed inhibition of luciferase activity, indicating that miR-221-3p directly binds to the 3'-UTR of *PDZRN4* mRNA (*Figure 3C*).

Further investigation revealed that, compared with normal tissues, miR-221-3p is overexpressed in colon cancer tissues (*Figure 3D*). At this point in the investigation, to

confirm the presence of a regulation network, the miR-221-3p and *PDZRN4* 3'-UTR vector was transfected into 293T cells. The luciferase report assay showed that luciferase activity was dose-dependent with miR-221-3p (*Figure 3E*), and this was true also for *PDZRN4* protein based on the western blot (*Figure 3F*). These results indicated the direct inhibition of *PDZRN4* expression by miR-221-3p.

To specify the binding sequence, we mutated several bases in both miR-221-3p and the *PDZRN4* 3'-UTR (*Figure 3G*). According to the dual luciferase assay, mutation in either miRNA or the *PDZRN4* 3'-UTR attenuated regulation (*Figure 3H*), and western blot was consistent with this (*Figure 3I*). These data indicated that the mutant regions of miR-221-3p and the *PDZRN4* 3'-UTR are the binding sites of this miR-3' UTR regulation system (*Figure 3G*).

Knockdown of miR-221-3p restrained tumorigenesis of HCT116 cells

To support that miR-221-3p-regulated *PDZRN4* expression interfered with the activity of colon cancer cells, miR-221-3p was knocked down by transducing HCT116 cells with a miRNA sponge. Observation and FACS detection of red fluorescent protein revealed that miR-221-3p was successfully dysregulated in HCT116 cells (*Figure 4A,B*). In addition, consistent with the results of miRNA overexpression, the levels of *PDZRN4* protein were comparable with that observed prior to knockdown of miR-221-3p (*Figure 4C*).

We then conducted more assays of phenotype. Both the cell proliferation (*Figure 4D*) and plate clone formation (*Figure 4E,F*) assays indicated that suppression of miR-221-3p expression lowered the proliferation of HCT116 cells. In addition, observations of the cell cycle showed inhibition of cell cycle progression (*Figure 4G,H*). Together, these data indicate that miR-221-3p functions in regulating HCT116 cell proliferation.

Moreover, the transwell migration, invasion, and wound-healing assays showed intense inhibition of cancer cell dissemination after treatment with the miR-221-3p sponge (*Figure 4I,J,K,L*). Together, these data indicate that miR-221-3p modulated the dissemination of colon cancer HCT116 cells.

Discussion

Gene dysregulation is a feature of cancer development. Various dysregulated genes may function as either tumor

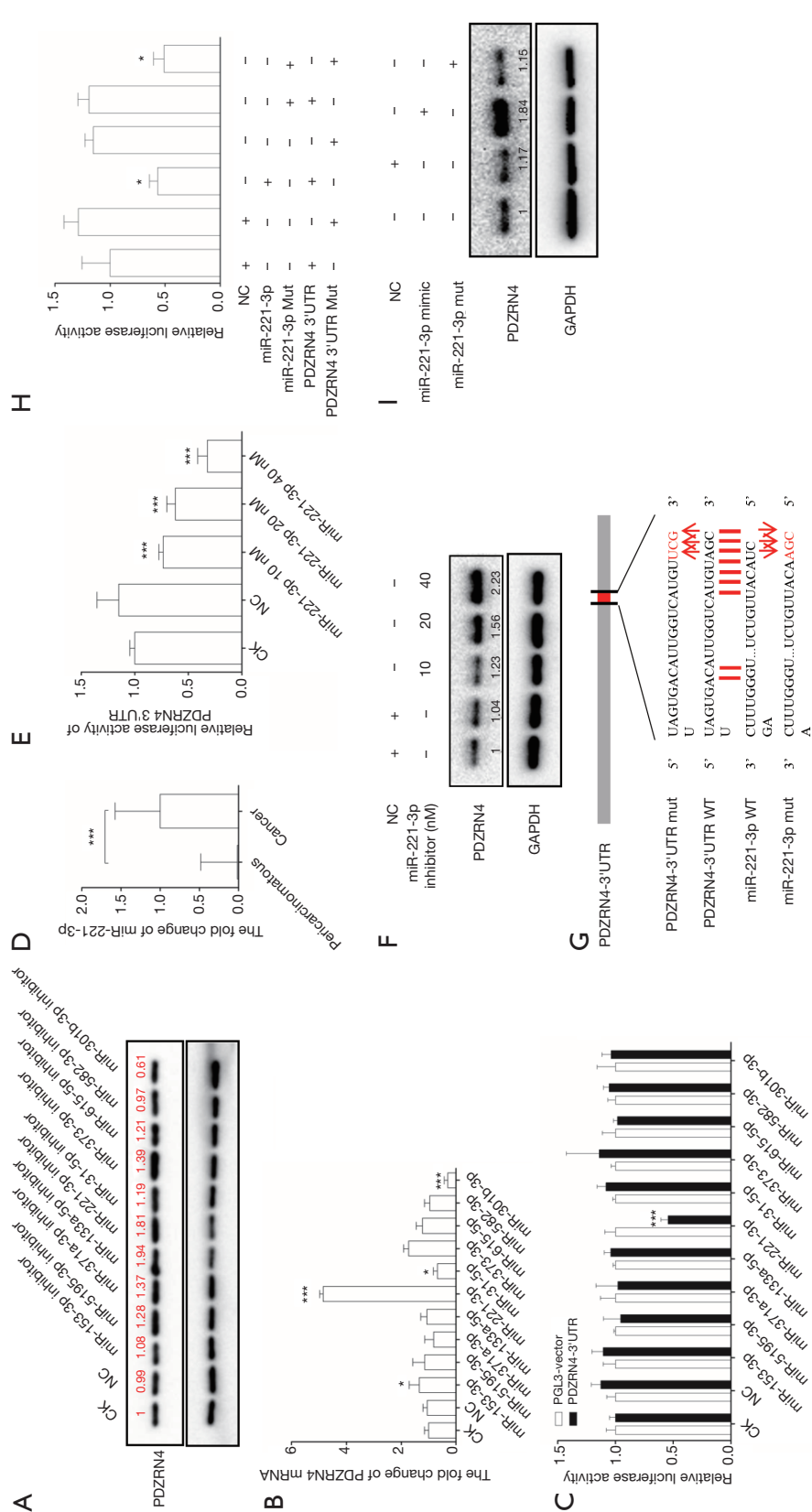
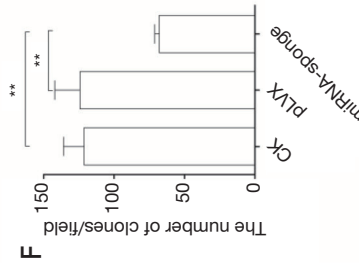
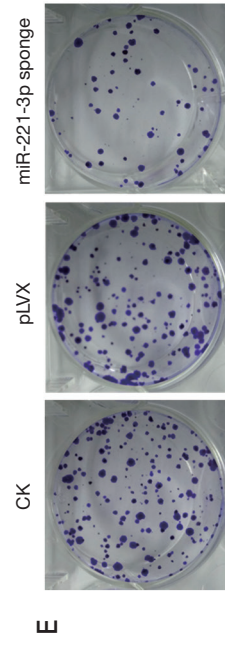
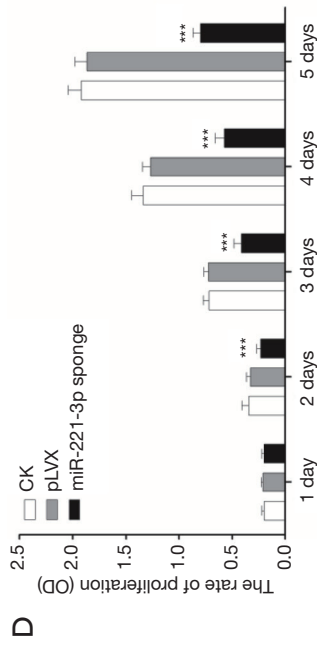
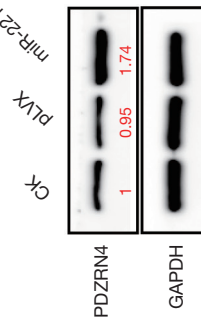
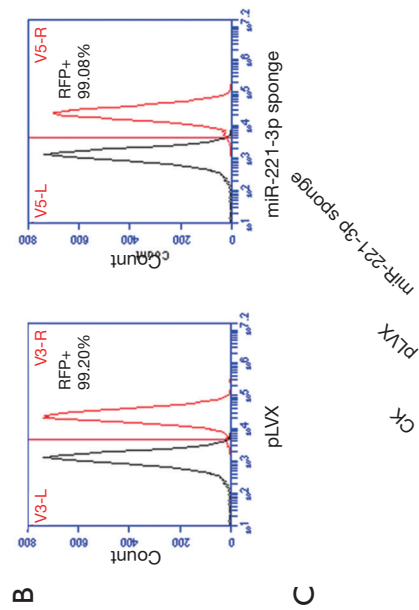
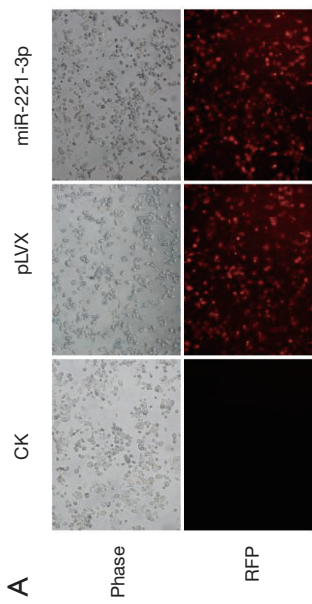


Figure 3 An overexpressed miRNA in colon cancer, miR-221-3p, directly targets PDZRN4. (A) Transfection of different miRNA inhibitors in 293T cells regulates PDZRN4 protein levels. (B) PDZRN4 mRNA in cells treated as in *Figure 3A*. *P<0.05, ***P<0.001 for Student's *t*-test. (C) Luciferase activity was detected in HCT116 cells co-transfected with different miRNAs. ***P<0.001 for Student's *t*-test. (D) miR-221-3p is upregulated in colon cancer tissues. ***P<0.001 for Student's *t*-test. (E) miR-221-3p regulated luciferase activity in a dose-dependent manner. ***P<0.001 for Student's *t*-test. (F) miR-221-3p inhibited PDZRN4 expression in a dose-dependent manner at the protein level. (G) Schematic illustration of the putative seed sequences of miR-221-3p complementary with PDZRN4 3'-UTR, and mutagenesis of binding sites in the 3'-UTR of PDZRN4 and miR-221-3p. (H) Luciferase activity was analyzed in HEK 293T cells co-transfected with miR-221-3p or miR-221-3p Mut, and PDZRN4 3'-UTR or PDZRN4 3'-UTR Mut. *P<0.05 for Student's *t*-test. (I) miR-221-3p failed to regulate endogenous PDZRN4 expression. HCT116 cells were transfected with NC, miR-221-3p mimic, or miR-221-3p mut and western blot was conducted 48 hours after transfection.



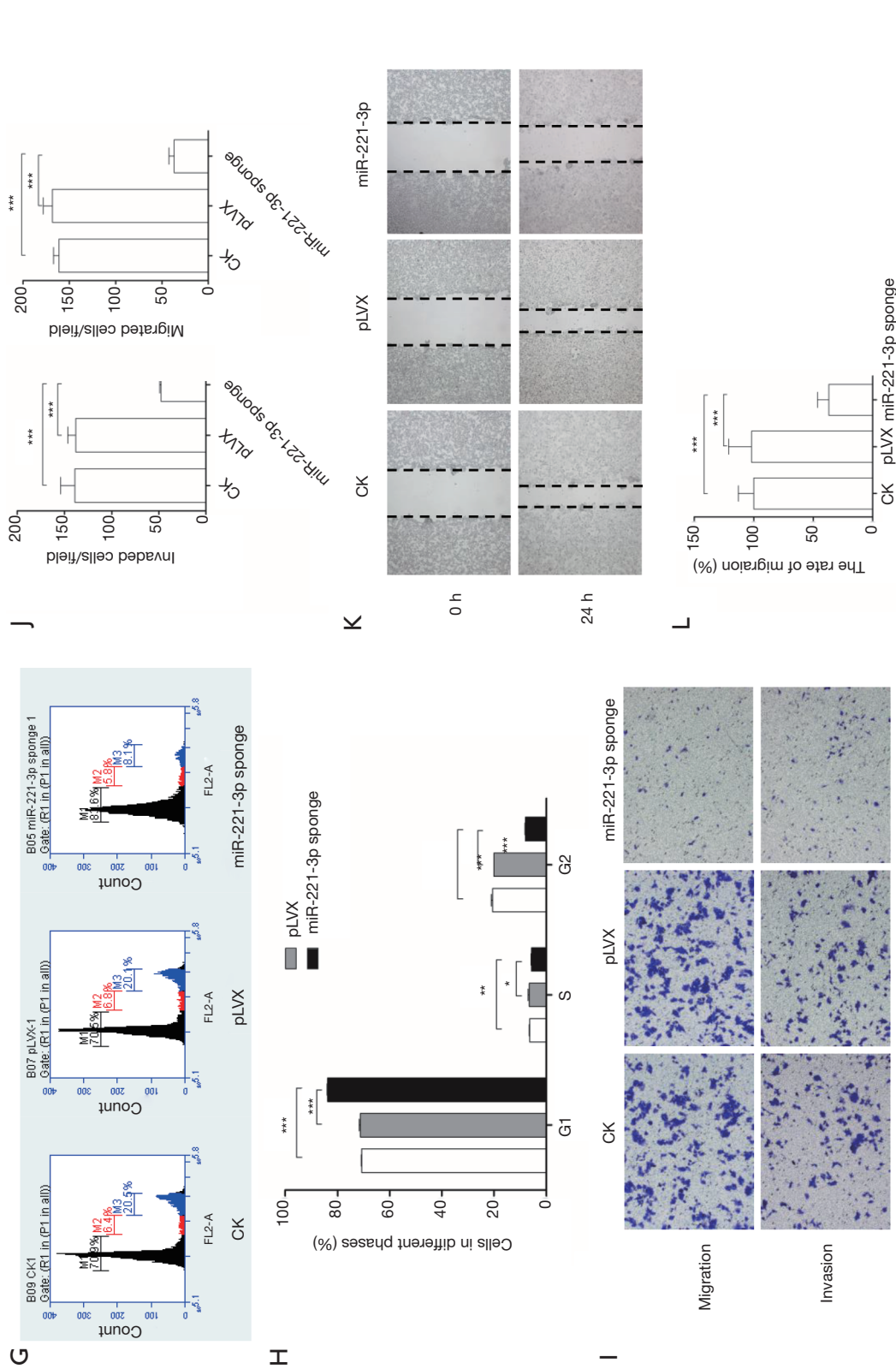


Figure 4 Knockout of miR-221-3p expression attenuated the proliferation, migration, and invasion of HCT116 cells. (A) HCT116 cells were transfected with a pLVX empty vector or miR-221-3p sponge lentivirus. Representative images of untreated cells (left) and transfected cells were taken under (Phase, top) light microscope, and (red fluorescent protein, bottom) fluorescent microscope (100 \times). (B) Percentage of cells treated as in *Figure 4A* tested positive for GFP by FACS. (C) PDZRN4 protein in HCT116 cells treated as in *Figure 4A*. (D) Proliferation of cells treated as *Figure 4A* by cell proliferation assay. *** $P < 0.001$ for Student's *t*-test. (E) Representative images taken for the clone formation of cells treated as *Figure 4A*. (F) Numbers of clones formed in *Figure 4A*. ** $P < 0.01$ for Student's *t*-test. (G) Percentage of cells treated as *Figure 4A* in different cell cycle phase. * $P < 0.05$, ** $P < 0.001$ for Student's *t*-test. (H) Number of migrated and invaded cells per field. *** $P < 0.001$ for Student's *t*-test. (I) Representative images for transwell migration and invasion of cells treated as *Figure 4A* (100 \times). (J) Percentages of migrated and invaded cells per field. *** $P < 0.001$ for Student's *t*-test. (K) Representative images of wound healing assay for cells treated as *Figure 4A* ($\times 100$). (L) Percentages of wound closure. *** $P < 0.001$ for Student's *t*-test.

suppressors or oncogenes. Thus, we searched and analyzed gene expression profiles, and chose an inhibited gene in colon cancer for further investigation, i.e., *PDZRN4*. The *PDZRN4* mRNA and PDZRN4 protein levels in colon cancer tissues were much lower than that of the adjacent normal tissues. Overexpressed *PDZRN4* in the colon cancer cell line arrested cell cycle, inhibited cell proliferation, and attenuated migration and invasion. This suggests that PDZRN4 protein in colon cancer tissues is negatively associated with cancer cell dissemination, and *PDZRN4* may function as a tumor suppressor in colon cancer development.

Furthermore, we found that *PDZRN4* translation was inhibited by an overexpressed onco-miRNA, miR-221-3p. The luciferase report assay showed a direct association between miR-221-3p and the 3'-UTR of *PDZRN4* mRNA. In addition, the cell proliferation and plate clone formation assays showed that as the miR-221-3p level subsided, so did the proliferation and dissemination of the colon cancer cell. This indicates that miR-221-3p-*PDZRN4* has an important role in regulating colon cancer development, in which miR-221-3p inhibits the translation of *PDZRN4* and thereby promotes the proliferation and dissemination of colon cancer cells.

In this study, the low number of clinical samples and time allowed limited sufficient inspection *PDZRN4* expression in colon cancer tissues. Whether *PDZRN4* protein is a viable biomarker of colon cancer requires further investigation.

Conclusions

This study investigated the expression of *PDZRN4* in colon cancer tissues, its potential function in the development of colon cancer, and its inhibition by its upstream regulator, miR-221-3p. Three main conclusions are highlighted. First, according to the gene expression profile and detection in clinical colon cancer samples, *PDZRN4* mRNA and PDZRN4 protein are downregulated in colon cancer. Second, overexpression of *PDZRN4* in the colon cancer cell line and the phenotype assays indicated that *PDZRN4* functions to attenuate cell proliferation, migration, and invasion. Thirdly, miR-221-3p inhibited *PDZRN4* translation by binding to its mRNA 3'-UTR. The knockdown of miR-221-3p dramatically reduced the proliferation, migration, and invasion of colon cancer HCT116 cells.

These discoveries suggest that *PDZRN4* may be a potential target for defeating colon cancer, but more

investigations are necessary.

Acknowledgments

Funding: This research was supported by the Suzhou Key Medical Center (LCZX201505, 2016.01-2018.12); the 2016 Suzhou Science and Technology Development Project (SZS201618, 2016.07-2019.06); the Jiangsu Provincial Commission of Health and Family Planning Foundation Project (CXTDA2017016, 2016.01-2020.12), the Second Affiliated Hospital of Soochow University Preponderant Clinic Discipline Group Project Fund, and the National Natural Science Foundation of China (81672970, 2017.01-2020.12).

Footnote

Conflicts of Interest: All authors have completed the ICMJE uniform disclosure form (available at <http://dx.doi.org/10.21037/tcr.2019.07.12>). The authors have no conflicts of interest to declare.

Ethical Statement: The authors are accountable for all aspects of the work in ensuring that questions related to the accuracy or integrity of any part of the work are appropriately investigated and resolved. The Institutional Ethics Committee of Second Affiliated Hospital of Soochow University (Suzhou, 215004, Jiangsu Province, China) reviewed and authorized the clinical section of this research. The study was conducted in accordance with the Declaration of Helsinki (as revised in 2013). Informed consent was taken from all patients.

Open Access Statement: This is an Open Access article distributed in accordance with the Creative Commons Attribution-NonCommercial-NoDerivs 4.0 International License (CC BY-NC-ND 4.0), which permits the non-commercial replication and distribution of the article with the strict proviso that no changes or edits are made and the original work is properly cited (including links to both the formal publication through the relevant DOI and the license). See: <https://creativecommons.org/licenses/by-nc-nd/4.0/>.

References

1. Brouwer NPM, Bos ACRK, Lemmens VEPP, et al. An overview of 25 years of incidence, treatment and outcome of colorectal cancer patients. *Int J Cancer*

- 2018;143:2758-66.
2. Zhang Y, Shi J, Huang H, et al. Burden of colorectal cancer in China. *Zhonghua Liu Xing Bing Xue Za Zhi* 2015;36:709-14.
 3. Poelmeijer YQM, Lijftogt N, Detering R, et al. Obesity as a determinant of perioperative and postoperative outcome in patients following colorectal cancer surgery: A population-based study (2009-2016). *Eur J Surg Oncol* 2018;44:1849-57.
 4. Pang Y, Kartsonaki C, Guo Y, et al. Diabetes, plasma glucose and incidence of colorectal cancer in Chinese adults: a prospective study of 0.5 million people. *J Epidemiol Community Health* 2018;72:919-25.
 5. Stein L, Rothschild J, Luce J, et al. Copy number and gene expression alterations in radiation-induced papillary thyroid carcinoma from chernobyl pediatric patients. *Thyroid* 2010;20:475-87.
 6. Hua Y, Ma X, Liu X, et al. Abnormal expression of mRNA, microRNA alteration and aberrant DNA methylation patterns in rectal adenocarcinoma. *PLoS One* 2017;12:e017446.
 7. Hu T, Yang H, Han ZG. PDZRN4 acts as a suppressor of cell proliferation in human liver cancer cell lines. *Cell Biochem Funct* 2015;33:443-9.
 8. Andres SF, Williams KN, Plesset JB, et al. IMP1 3' UTR shortening enhances metastatic burden in colorectal cancer. *Carcinogenesis* 2019;40:569-79.
 9. Wang T, Hou J, Jian S, et al. miR-29b negatively regulates MMP2 to impact gastric cancer development by suppress gastric cancer cell migration and tumor growth. *J Cancer* 2018;9:3776-86.
 10. Yu L, Xiang L, Feng J, et al. miRNA-21 and miRNA-223 expression signature as a predictor for lymph node metastasis, distant metastasis and survival in kidney renal clear cell carcinoma. *J Cancer* 2018;9:3651-9.
 11. Xie X, Huang Y, Chen L, et al. miR-221 regulates proliferation and apoptosis of ovarian cancer cells by targeting BMF. *Oncol Lett* 2018;16:6697-704.
 12. Yang Y, Li H, Ma Y, et al. MiR-221-3p is down-regulated in preeclampsia and affects trophoblast growth, invasion and migration partly via targeting thrombospondin 2. *Biomed Pharmacother* 2019;109:127-34.
 13. Zheng X, Dai J, Zhang H, et al. MicroRNA-221 promotes cell proliferation, migration, and differentiation by regulation of ZFPM2 in osteoblasts. *Braz J Med Biol Res* 2018;51:e7574.
 14. Cai K, Shen F, Cui JH, et al. Expression of miR-221 in colon cancer correlates with prognosis. *Int J Clin Exp Med* 2015;8:2794-8.
 15. Tao K, Yang J, Guo Z, et al. Prognostic value of miR-221-3p, miR-342-3p and miR-491-5p expression in colon cancer. *Am J Transl Res* 2014;6:391-401.
 16. Liu S, Sun X, Wang M, et al. A microRNA 221- and 222-mediated feedback loop maintains constitutive activation of NFκB and STAT3 in colorectal cancer cells. *Gastroenterology* 2014;147:847-59.e11.
 17. Tsunoda T, Takashima Y, Yoshida Y, et al. Oncogenic KRAS regulates miR-200c and miR-221/222 in a 3D-specific manner in colorectal cancer cells. *Anticancer Res* 2011;31:2453-9.
 18. Moshiri F, Callegari E, D'Abundo L, et al. Inhibiting the oncogenic mir-221 by microRNA sponge: toward microRNA-based therapeutics for hepatocellular carcinoma. *Gastroenterol Hepatol Bed Bench* 2014;7:43-54.

Cite this article as: Liu X, Xing C. *PDZRN4*-mediated colon cancer cell proliferation and dissemination is regulated by miR-221-3p. *Transl Cancer Res* 2019;8(4):1289-1300. doi: 10.21037/tcr.2019.07.12

Supplementary**Table S1** Patient information enrolled in research

Patient No.	Gender	Age, years	Histological type	LNM	Tumor size, cm ³
PT 1	F	64	Mucinous adenocarcinoma	POS	3.5×4.5×1.5
PT 2	M	75	Canalicular adenoma	POS	8.0×5.5×2.5
PT 3	F	83	Signet-ring cell carcinoma	POS	7.0×4.5×2.0
PT 4	M	79	Mucinous adenocarcinoma	POS	5.0×4.0×2.3
PT 5	M	63	Canalicular adenoma	POS	3.5×2.0×1.0
PT 6	F	37	Canalicular adenoma	POS	5.0×4.5×2.0
PT 7	F	85	Canalicular adenoma	NEG	4.0×4.0×1.0
PT 8	M	51	Signet-ring cell carcinoma	POS	6.0×2.5×2.0
PT 9	F	84	Canalicular adenoma	NEG	10.0×5.0×4.5
PT 10	M	73	Canalicular adenoma	NEG	5.5×3.5×2.0
PT 11	M	74	Canalicular adenoma	POS	4.0×3.3×1.5
PT 12	F	55	Canalicular adenoma	NEG	1.1×0.9×0.5
PT 13	F	58	Canalicular adenoma	POS	6.5×4.0×3.0
PT 14	F	74	Mucinous adenocarcinoma	POS	3.5×2.0×1.5
PT 15	M	64	Polypoid adenocarcinoma	POS	3.0×2.2×1.6
PT 16	M	60	Canalicular adenoma	POS	4.3×3.2×1.5
PT 17	F	70	Canalicular adenoma	POS	8.0×5.0×2.5
PT 18	F	58	Canalicular adenoma	POS	6.0×3.5×2.0
PT 19	M	71	Canalicular adenoma	POS	3.2×3.0×0.8
PT 20	M	78	Canalicular adenoma	POS	6.0×4.0×4.0

F, female; LNM, lymph node metastasis; M, male; NEG, negative; POS, positive; PT, patient.

VIP	PPP1R14A	ADAMTS8	CNRIP1	PTN	CCL21
RERGL	MFAP5	PPP2R2B	FERMT2	SGCE	FGL2
MYH11	PTGS1	NEXN	DDR2	ANTXR2	KCNMB1
DES	SPARCL1	MEIS1	MEIS2	ANGPTL1	PDE5A
C7	LMOD1	SYNC	PRUNE2	HSPB3	SPEG
PGM5	LPAR1	SYT4	PODN	TSHZ3	GCNT2
CNN1	STMN2	GPM6A	PDLIM3	FCER1A	AFF3
MYOM1	RUNDC3B	ADHFE1	SGCA	SMARCD3	GNAO1
CFD	STOX2	JAM2	ATP2B4	LMOD3	PTCHD1
RBPMS2	CDH19	SMYD1	RERG	EIF4E3	POPCD2
ATP1A2	MYOT	SLC9A9	GREM2	TBC1D9	SMTN
FHL1	RGMA	PRRT2	EBF1	ANKS1B	MMRN1
CLEC3B	SETBP1	FOSB	CASZ1	ARMCX1	TAGLN
MAMDC2	ACACB	AHNAK	PLN	CAP2	TACR2
ABCA8	DACT3	SLC25A23	TAGLN3	MRGPRF	CYBRD1
DPT	SRPX	SLIT2	ELAVL4	BNC2	ANK2
NPTX1	FXYD6	LYVE1	MAF	SLC6A16	P2RX1
PRPH	GNG7	TEF	MASP1	RPRM	COLEC12
SCARA5	LIMS2	PLEKHO1	HSPA2	LRRFIP1	TMOD1
HAND1	CD209	CITED2	KCNN3	ARRDC4	CACNA1H
RNF150	NNAT	CNTFR	ETFDH	REEP1	MXI1
CASQ2	GSN	PALM	MAP1B	FMN2	GPR162
HSPB6	PLP1	ZSCAN18	EMP3	OPTN	JPH2
PLAC9	ADH1B	SCN9A	AGTR1	LDB3	SLIT3
CXCL12	SCG2	PCP4	ADAMTS1	OLFML1	FOLR2
ADH1A	PI16	CBX7	TSPAN18	ZNF671	SLC22A17
LRRN2	FNBP1	PINK1	KIAA1683	ADAMTSL3	A2M
FAM107A	PCOLCE2	PDZD4	CSF1R	VIPR2	ADCY9
CKB	FLNA	BCHE	STBD1	SCUBE2	TPM1
PDE9A	PDE7B	NLGN1	REEP2	PMP22	CBX6
ACTG2	FXYD1	SORBS2	OLFML2A	GFRA3	MAOB
SEMA6A	IGFBP6	HTR4	SPECC1L	NGB	DIXDC1
MYLK	FOXF2	PDZRN4	GSTM2	LGI4	RASGRP2
SCGN	TSC22D3	KIAA0513	AXL	SYNGR1	UCHL1
C2orf40	TMEM100	TCN2	GSTM5	TGFB111	DENND5B
PNCK	PEG3	SNAP91	ARHGEF37	SALL2	CELF2
PKD4	SORBS1	GLIPR2	RGL1	DAAM2	RCSD1
GPX3	THBS4	MS4A7	MYOC	LINC00341	CSPG4
CRYAB	CLIP3	RELN	GLI3	DSEL	CLMP
HSPB8	MGP	PTH1R	FAM189A2	ROR2	CBLN2
NPY	STAB1	KCNMA1	F13A1	KCNH2	EML1
METTL7A	XKR4	TGFBR3	LRCH2	PPP2R3A	DDAH2
TCEAL2	KIF1A	BOC	KIT	CHODL	LPP
ABI3BP	LIFR	PSG11	TRIM9	SGCD	CHST15
MFAP4	FAM46B	PDGFRA	PTRF	FGF13	KCNIP3
GFRA2	CPXM2	KANK2	SSBP2	CCDC136	SNAP25
ZBTB16	CSRP1	MEF2C	TNFSF12	ANKRD35	GYPC
SDPR	COX7A1	C15orf52	KCNA5	SOBP	OGN
GABARAPL1					

Figure S1 Upregulated genes in both arrays (by acronym).

SLC38A5	CNPY2	KNTC1	JPH1	HSPD1	PSAT1
DACH1	ANKRD22	UBD	TIMELESS	CCNO	HMMR
CHPF	TOP1MT	FBL	MCM7	EEF1E1	PUS7
OLR1	KPNA2	KCTD14	HSPH1	SLC6A14	CCNB2
BLM	C4BPB	EZH2	FAM84B	TROAP	ITGA2
NCAPD2	EPHB2	CFB	CST1	GNL3	KIAA0101
NIPSNAP1	RANGAP1	CDCA8	SULT2B1	ASF1B	TESC
GJB3	POLE2	GSTO2	HES6	MYEOV	NCAPG
RECQL4	CECR5	KIF14	IL24	SALL4	AURKA
DARS2	C10orf2	SPAG5	NUP37	MMP10	NME1
RHBDF2	TMEM63A	METTL1	CDT1	RPS21	NUSAP1
AZGP1	LIPG	SH3BP4	CENPE	GDF15	TMEM97
RFWD3	KLHL35	NOP16	EBPL	LMNB2	MCM4
SPC25	MCM10	NUP62CL	SHMT2	LRP8	UBE2T
BRCA1	HPRT1	SKA3	EPHB3	TYMS	CENPN
GGCT	E2F7	DDIT4	MET	RAD51AP1	CENPF
DUSP4	FOXM1	NDC80	POLQ	TK1	GIN52
ICA1	CENPK	ZWINT	GPT2	PAQR4	MAD2L1
CXCL10	NUDT5	RFC5	KIF4A	MCM2	TRIB3
GMNN	KCNN4	MND1	RTKN	CELSR3	SCD
ZNF593	PAFAH1B3	MLXIPL	KIF11	PBK	PAICS
MRPS12	HMGB3	ANAPC1	IL17RB	SPINK1	CTHRC1
GPX2	EARS2	CHTF18	DHCR7	C19orf48	PTTG1
SRPRB	FAM64A	KLK6	CKAP2L	TEAD4	IQGAP3
MIPEP	MMP12	IFITM1	PCNA	MMP11	SERPINB5
NOB1	ATIC	BYSL	AURKB	ENC1	KRT80
GMDS	BORA	WDR4	FERMT1	MELK	CLDN2
SQLE	YARS2	PODXL2	KIF2C	CENPA	TRIP13
DIO2	SF3B3	STIL	MARCKSL1	CENPW	SOX9
KIF23	TMPRSS3	FANCD2	TGIF1	BUB1B	TPX2
PAM16	IL1RN	PLEK2	RAD54L	PYCR1	PRC1
RPIA	RCC2	REEP6	FANCI	NEBL	CKS2
SLC1A5	SRPK1	ECE2	CBX2	S100P	CDC20
TGDS	TSMF	SLC25A15	S100A11	RNF43	CEP55
RAD54B	CDC45	MTHFD2	KIF15	KRT6B	ASPM
SLC16A10	FAM57A	GART	POLR1C	KIF20A	SLCO4A1
CHD7	SYBU	OLFM4	GGH	DKC1	CDH3
NCAPD3	RUVBL2	PLAU	IMPDH2	CCNB1	REG1B
BACE2	SLC12A8	CMTM8	HJURP	NFE2L3	CXCL1
TBRG4	E2F5	RRP9	PPAT	HOXB8	TOP2A
KRTCAP3	SLC25A22	NUF2	PRDX4	BUB1	CDCA7
MTHFD1	CCNF	GNPNAT1	EXO1	CCNA2	ASCL2
AEN	FUT4	RMI2	SNRPF	CDCA3	MMP1
FBXO5	ZDHHC9	SLC29A2	PUS1	DLGAP5	REG1A
FABP6	C16orf59	FOXA2	WDR12	DPEP1	CLDN1
OIP5	NOP56	KLK11	TOMM34	TTK	MMP7
RPA3	CHAF1B	CDC25A	FASN	SLC12A2	FOXQ1
PKMYT1	F12	RAB15	SOX4	CDKN3	UHRF1
IRX2	FAM60A	PLK4	LCN2		

Figure S2 Downregulated genes in both arrays.